J. Biochem. 124, 28-34 (1998)

Stable Isotope-Edited NMR Analysis of *Ascaris suum* Mitochondrial tRNA^{Met} Having a TV-Replacement Loop[1]

Takashi Ohtsuki, Gota Kawai, and Kimitsuna Watanabe[2]

Department of Chemistry and Biotechnology, Graduate School of Engineering, The University of Tokyo, 7-3-1 Hongo, Bunkyo-ku, Tokyo 113-8656

Received for publication, December 2, 1997

Most nematode mitochondrial (mt) tRNAs have a TV-replacement loop (TV loop) which replaces the normal T arm and the variable loop in standard tRNAs with a less-structured loop. The tertiary structure of such tRNAs has been discussed theoretically with reference to the crystal structure of yeast tRNA^{Phe} [Wolstenholme *et al.* (1994) *Nucleic Acids Res.* 22, 4300-4306] and examined experimentally by chemical and enzymatic probing [Watanabe *et al.* (1994) *J. Biol. Chem.* 269, 22902-22906]. The results suggest that most regions of the tRNA other than the TV loop are folded in a similar manner to yeast tRNA^{Phe}. To confirm this notion more clearly, the tertiary structure of *Ascaris suum* mt tRNA^{Met} was analyzed by NMR using various synthetic tRNAs site-specifically labeled with stable isotopes, which were prepared by a combination of chemical synthesis and enzymatic ligation. Tertiary interactions involving G(L2), G(L3), U(L4), and U8 were observed in the NMR spectra of the labeled tRNAs, but those relating to G(L5) were not. On the basis of these results, a possible tertiary structural model of nematode mitochondrial tRNA^{Met} was constructed.

Key words: mitochondria, nematode, NMR, stable isotope, tRNA.

All prokaryotic and eukaryotic cytoplasmic tRNAs are folded into a similar cloverleaf secondary structure (*1*). In contrast to these standard tRNAs, many metazoan mitochondrial (mt) tRNAs cannot take the canonical cloverleaf form because they lack some conserved nucleotides common to standard tRNAs; the D arm is replaced with a simple loop in most metazoan mt tRNAs$^{Ser}_{GCU}$ (*1*), and almost all nematode mt tRNAs have a TV-replacement loop (TV loop) consisting of 4-12 nucleotides, which replaces the T arm and the variable loop in standard tRNAs (*2-5*). In mitochondria of *Ascaris suum* and *Caenorhabditis elegans*, 22 tRNA genes are encoded in the mt genomes but none of them can be folded into the canonical cloverleaf form; 20 tRNAs lack the T stem, and both tRNA$^{Ser}_{UCU}$ and tRNA$^{Ser}_{UCA}$ lack the D stem, as inferred from their DNA sequences (*6*). Transcripts corresponding to some of these nematode mt tRNA genes have been detected by Northern blot analysis (*3, 5*) as well as by direct RNA sequencing (*5, 7*), demonstrating that tRNAs with unusual secondary structures in fact exist in nematode mitochondria.

In most of metazoan mitochondria, tRNAs$^{Ser}_{GCU}$ lacking the D arm coexist with tRNAs possessing the nearly canonical cloverleaf structure, and as a result they should be recognized in a similar manner to standard tRNAs by mt elongation factor Tu (EF-Tu) and ribosomes, because it is assumed that tRNAs$^{Ser}_{GCU}$ probably take a nearly L-shaped form as a whole due to structural compensation occurring within mt tRNA molecules (*8*). On the other hand, the situation is quite different for nematode mt tRNAs, because none of them can be folded into the canonical cloverleaf form. It is assumed that a unique EF-Tu specific for these unusually structured tRNAs exists in nematode mitochondria (Watanabe *et al.*, submitted); the EF-Tu possesses a C-terminal extended sequence consisting of 60 amino acid residues, which is speculated to function so as to compensate for the lacking or truncated T arm region. In this regard, information on the tertiary structure of these nematode mt tRNAs may provide a clue to answering such questions as whether these tRNA function like standard tRNAs and how they are recognized by EF-Tu.

By referring to the crystal structure of yeast tRNA^{Phe} (*9*), the tertiary interactions in nematode mt tRNAs have been inferred, mainly from their gene sequences (*10*). Although three sets of binary combinations relating to the T loop common to standard tRNAs (G18-Ψ55, G19-C56, and T54-A58) are not present in *A. suum* and *C. elegans* mt tRNAs, the other five commonly existing sets of binary and ternary combinations seem to be conserved as shown in Fig. 1. These observations led to the speculation that even such unusual tRNAs as those lacking the T stem can be folded into an L-shape-like structure roughly similar to those of standard tRNAs, except for the TV loop region (*10*). This speculation has been supported by the enzymatic and chemical probing of several *A. suum* mt tRNAs (*5*). In the present study, the interactions between the TV loop and

[1] This work was supported by Grants-in-Aid for Scientific Research on Priority Areas (Nos. 04272102 and 04272103) from the Ministry of Education, Science, Sports and Culture of Japan, JSPS (to T.O.) and by the Human Frontier Science Program Organization.

[2] To whom correspondence should be addressed.

Abbreviations: BAP, *E. coli* alkaline phosphatase; EF-Tu, elongation factor Tu; HMQC, heteronuclear multiple quantum correlation; mt, mitochondrial; PEG, polyethylene glycol; TV loop, TV-replacement loop.

some other regions were elucidated by means of NMR spectroscopy.

Recently, NMR analysis of RNA molecules has been greatly improved, and a number of RNA structures have been elucidated by this means (*11*). The improvement mainly results from the introduction of an *in vitro* transcription system with T7 RNA polymerase (*12*) and stable isotopic labeling (*13-15*) for the preparation of RNA samples suitable for NMR measurement. *In vitro* transcription with NTP labeled with stable isotopes has enabled the production of large amounts of labeled RNA samples with desired sequences. However, a further technique is also needed for site-specific labeling. Hence, we introduced a selective labeling technique to analyze the *A. suum* mt $tRNA^{Met}$.

We previously prepared *A. suum* mt $tRNA^{Met}$ by the enzymatic ligation of chemically synthesized RNA fragments (*16*). Although the synthetic tRNA had no modified nucleosides, such as Ψ3, m^1A9, m^2G26, Ψ27, f^5C34, and Ψ71, which exist in native $tRNA^{Met}$, the aminoacylation activity and the enzymatic probing of the synthetic tRNA both provided good evidence that the synthetic $tRNA^{Met}$ possesses a very similar tertiary structure to the native one (*16*).

In this work, synthetic $tRNAs^{Met}$ site-specifically labeled with stable-isotopes were prepared by the enzymatic ligation of RNA fragments and labeled mono- or dinucleotides, in which the nucleotide residues in the TV loop assumed to be involved in the tertiary interactions could be labeled (Fig. 1). NMR measurement was focused on the labeled residues to examine their involvement in tertiary interactions.

MATERIALS AND METHODS

Preparation of Stable Isotopic Labeled Nucleotides—E. coli [^{15}N,^{13}C]rRNA was purchased from Nippon Sanso, Tsukuba. [^{15}N,^{13}C]3′-UMP (Up) and [^{15}N,^{13}C]GUp were obtained by RNase A digestion of [^{15}N,^{13}C]rRNA (60 mg), and [^{15}N,^{13}C]Gp was obtained by RNase T_1 digestion of [^{15}N,^{13}C]-rRNA (50 mg), as described previously (*17*).

TABLE I. **Summary of ligation reactions.**

Ligation[a]	Buffer[c]	PEG (%)	5′-RNA (μM)	3′-RNA (μM)	Ligase (unit/ml)	Purification method[d]	Yield[e] (%)
8-1	A	5	90	70	600	monoQ	50
8-2	A	5	70	70	600	PAGE	67
8-3[b]						PAGE	—
L2-1	A	5	90	90	1,000	monoQ	28
L2-2	A	0	60	60	600	monoQ	39
L2-3[b]						PAGE	—
L3-1	A	5	90	75	1,370	monoQ	80
L3-2	A	5	120	90	1,250	monoQ	43
L3-3[b]						monoQ	80
L5-1	A	5	90	90	750	PAGE	79
L5-2	B	5	60	60	600	PAGE	53
L5-3[b]						PAGE	76

[a]The numbering is shown in Fig. 2. [b]The reaction was performed as described (*16*). [c]Buffers: A: 50 mM Tris-HCl-15 mM $MgCl_2$-3.5 mM DTT-15 μg/ml BSA-300 μM ATP, pH 7.5; B: 50 mM Tris-HCl-10 mM $MgCl_2$-3.5 mM DTT-15 μg/ml BSA-300 μM ATP, pH 7.2. [d]monoQ: monoQ HR 5/5 column chromatography; PAGE: 10% denaturing (7 M urea) polyacrylamide gel electrophoresis. [e]Yield after purification; —: Data not obtained.

The products obtained by RNase A digestion were separated into monomer, dimer, trimer, and longer fractions on a DEAE-cellulose column (DE52; Whatmann) (1.5×42 cm) by use of a linear gradient of 0-0.3 M NaCl in 7 M urea-50 mM Tris-HCl pH 7.5 buffer (total 2 liters). [^{15}N,^{13}C]Up was purified from the monomer fraction on a Dowex-1 AG 1-X2 column (Bio-Rad) (1×40 cm) by use of a linear gradient of 0.004 N HCl buffer (250 ml) and 0.0075 N HCl-0.09 M NaCl buffer (250 ml). [^{15}N,^{13}C]GUp was purified from the dimer fraction on a Dowex-1 AG 1-X2 column (1×40 cm) by elution using a gradient of 400 ml of 0.004 N HCl buffer and 600 ml of 0.01 N HCl-0.45 M NaCl buffer. [^{15}N,^{13}C]Gp (*i.e.* a monomer fraction) was purified from the products of RNase T_1 digestion using a DEAE-cellulose column as described above. After desalting on a DEAE-sephadex A-25 column (Pharmacia), the nucleotides were phosphorylated: 5′-phosphorylation was performed at 37°C for 3 h in a reaction mixture (100-1,000 μl) consisting of 1.0 mM nucleotide, 2.0 mM ATP, 50 mM Tris-HCl (pH 7.5), 10 mM $MgCl_2$, and 250 units/ml T4 polynucleotide kinase (3′-phosphatase free; Boehringer Mannheim). After the reaction, T4 polynucleotide kinase was removed using an ultrafilter (Ultra Free C3-GC, cut off 10,000 Da; Millipore).

Preparation of RNA Fragments Used for Ligation—RNA fragments were synthesized with an Applied Biosystems 381A DNA synthesizer. Deprotection and purification of the synthetic RNAs were performed as described (*16*). To enable the fragments to serve as substrates for the RNA ligase reaction, as well as to prevent self-ligation, both ends of 5′-fragments must be free of phosphate, and both ends of 3′-fragments must be phosphorylated. Phosphorylation of RNA fragments having OH at both ends was performed as described (*18*): the 5′-end was phosphorylated with T4 polynucleotide kinase (Toyobo), and the 3′-end was treated with $NaIO_4$ to remove the terminal nucleoside, resulting in the 3′-phosphorylated end. RNA fragments having a 3′-phosphate end were phosphorylated at the 5′-end using T4 polynucleotide kinase (3′-phosphatase free; Boehringer Mannheim) as previously described using T4 polynucleotide kinase possessing 3′-phosphatase activity (*16*). Deprivation of the phosphate group at both ends was accomplished using *E. coli* alkaline phosphatase (BAP) (Takara Shuzo). The reaction was carried out at 37°C for 30 min in a reaction mixture containing 300 μM RNA fragment, 25 mM Tris-HCl (pH 7.6), 5 mM $MgCl_2$, and 3 units/ml BAP. After the reaction, BAP was removed by phenol treatment followed by ethanol precipitation.

Ligation of RNA Fragments—The optimal conditions for the ligation reaction differ depending on the substrate. The conditions for each reaction shown in Fig. 2 are summarized in Table I. The reactions were performed at 11°C for 14-16 h. All the ligation reactions in the anticodon loop were carried out between A35 and U36. After preliminary

TABLE II. **Comparison of tertiary interactions observed in *A. suum* mt $tRNA^{Met}$ and yeast $tRNA^{Phe}$.**

A. suum mt $tRNA^{Met}$	Yeast $tRNA^{Phe}$ (*9*)
G(L2)-G10-C25	G45-G10-C25
G(L3)-G22-U13	G46-G22-C13
U(L4)-A15	C48-G15
U8-A14	U8-A14

Labeled nucleotides used in this study are underlined.

small-scale experiments using 40-50 μl of the reaction mixture to determine the optimal conditions, large-scale reactions were carried out. The buffer conditions, and the concentrations of polyethylene glycol #6000 (PEG), ligase, and the substrates were optimized. Slight degradation of the ligated RNA sometimes occurred when Buffer A was used, which was avoided by replacing Buffer A with Buffer B. When Buffer B lowered the efficiency of ligation, reducing the concentration of substrate RNA in Buffer A prevented the degradation without decreasing the efficiency.

The optimum concentration of PEG was generally around 5%, and that of the substrate RNA was about 90 μM in many cases; in some instances, lowering the substrate concentration to less than 90 μM raised the efficiency of the ligation reaction. The concentrations of labeled RNAs and RNA ligase were kept as low as possible without decreasing the reaction efficiency. The tRNAs thus obtained were finally purified by either monoQ HR 5/5 column (Pharmacia Biotech) chromatography or 10% denaturing (7 M urea) polyacrylamide gel electrophoresis.

NMR Spectroscopy—Each of the labeled tRNAs was dissolved in 200 μl of a buffer consisting of 10 mM sodium cacodylate (pH 6.0), 0.1 mM EDTA, 100 mM NaCl, and 5% ^2H_2O. The 500 MHz ^{1}H-NMR spectra were recorded on a Bruker AMX-500 spectrometer. The water signal was suppressed by a Jump-and-Return sequence (*19*). 1D spectra of [^{15}N]^{1}H heteronuclear multiple quantum correlation (HMQC) with ^{15}N,^{13}C-decoupling (*20*) were obtained with an interpulse delay time of 4 ms. Protons were decoupled from ^{15}N and ^{13}C during acquisition by a GARP sequence (*21*). Selective decoupling of ^{15}N was performed by continuous irradiation with a power of 25 dB below 300 W.

Model Building—The model was manipulated using the MidasPlus software system (*36*). Calculations and visualizations were performed using the Insight/Discover package (BIOSYM/Molecular Simulations). Modified bases were not taken into account throughout the modeling. Energy minimization (EM) and molecular dynamics (MD) calculations were performed by adding the aqueous solvent in the Discover module with an AMBER force field. All the manipulations and calculations were performed on a INDY R5000 workstation (Silicon Graphics).

The manipulation was performed as follows: (i) delete the "absent" residues, which means the residues 17, 47, and 52-61 present in yeast tRNA^{Phe}, but all of which are absent in *A. suum* mt tRNA^{Met}, from the yeast tRNA^{Phe} tertiary structure (*9*), (ii) move residues 16-19 and L6-L9 (corresponding to 50, 51, 62, and 63 in tRNA^{Phe}) so as to fill the gap formed by these deletion, (iii) replace the residues from tRNA^{Phe} with those of mt tRNA^{Met}, (iv) run calculations for EM and MD with base pair restraints. Tertiary hydrogen bondings shown in Table II and all the secondary hydrogen bondings were restrained in a manner such that the distance between a heavy atom and a proton should be 1.7 ± 0.2 Å, through the calculations. The tRNA structure was refined by 200 EM iterations followed by MD of 1 ps at 300 K and a further 200 EM iterations. MD calculation was performed for all regions except the anticodon arm and acceptor stem.

RESULTS

The nucleotide residues assumed to be involved in tertiary interactions (Fig. 1) were specifically labeled with stable isotopes of ^{15}N and ^{13}C (see "MATERIALS AND METHODS") by a combination of chemical synthesis and enzymatic ligation. To investigate the interactions between the TV loop and the D arm, residues G(L2)-G(L5) in the TV loop were labeled. As a result, four kinds of stable isotopic-labeled tRNAs were prepared (Fig. 2). The yield of each ligation reaction including the purification step is shown in Table I. The RNA fragments used for the ligation reactions were chemically synthesized at a scale of 1 or 2 μmol (using 1-μmol CPG-packed columns). From these RNA fragments, 1.4, 0.65, 1.5, and 3.2 mg of tRNAs labeled at positions U8, G(L2), G(L3)-U(L4), and U(L5), as shown by Fig. 2, a-d, respectively, were finally obtained.

The ^{15}N-decoupled 1D spectra of all the labeled tRNAs coincided well with the spectrum of non-labeled tRNA (Fig. 3d), indicating that ligation at different positions caused no appreciable difference in the tertiary folding of the tRNAs.

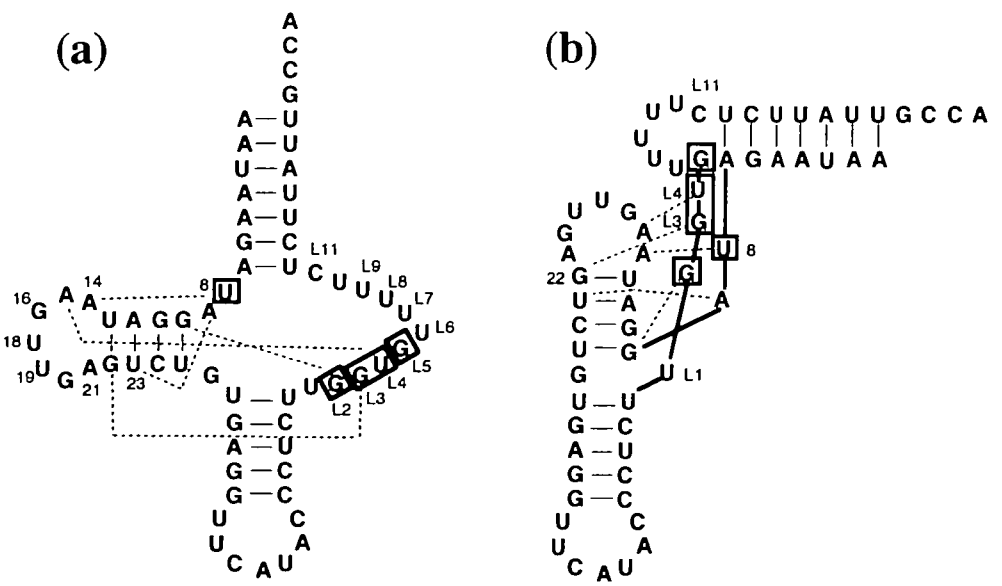

Fig. 1. **Secondary structure of *A. suum* mt tRNA^{Met} (a) and schematic depiction of its possible tertiary folding with tertiary interactions (b).** Residues labeled with stable isotopes are boxed. Dotted lines indicate the tertiary interactions proposed (*10*).

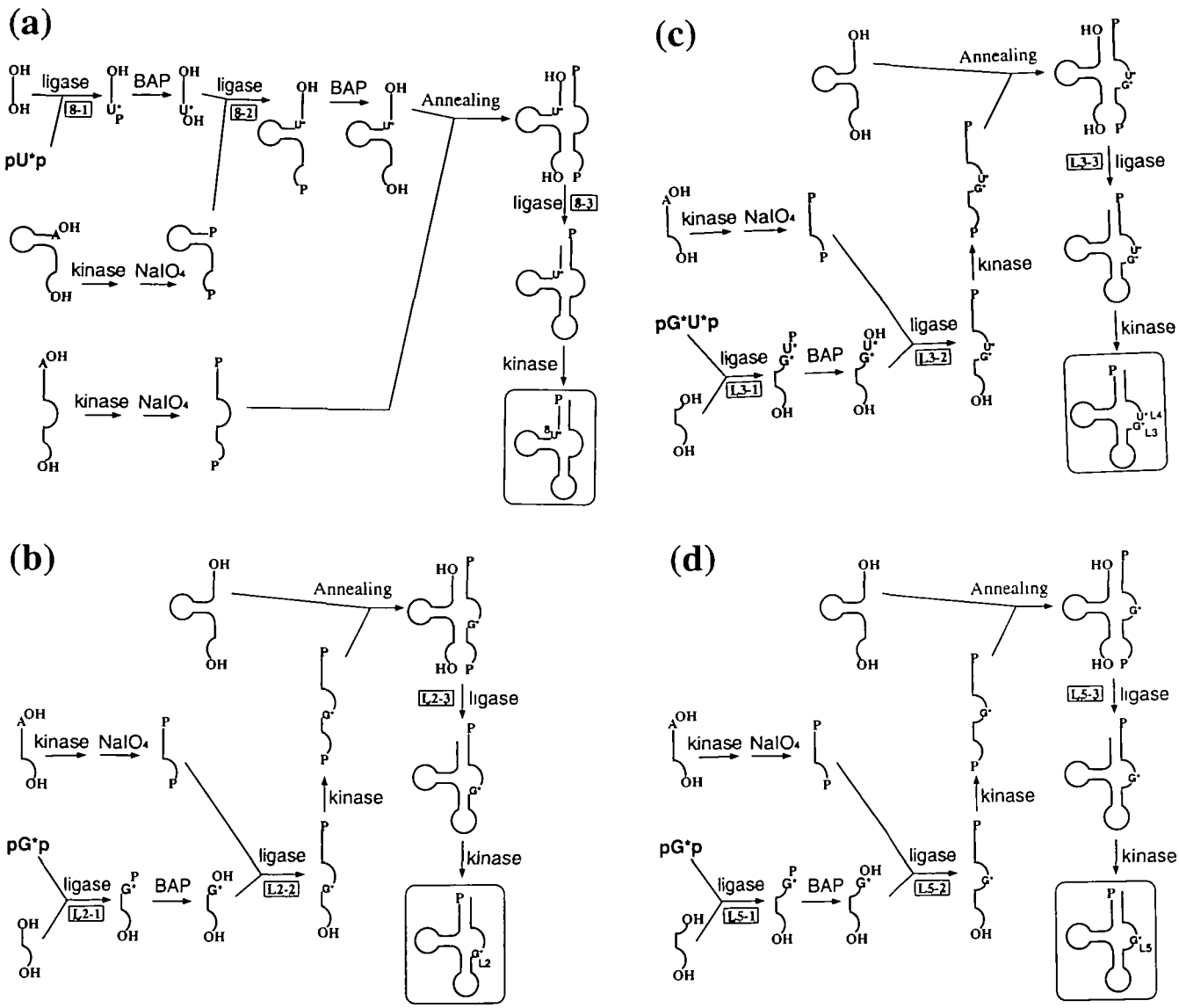

Fig. 2. **Diagrams showing how synthetic *A. suum* mt tRNAs^{Met} were constructed.** Individual residues [U8 (a), G(L2) (b), G(L3)-U(L4) (c), and G(L5) (d)] were labeled site-specifically with both ^{15}N- and ^{13}C-labeled nucleotides. Asterisks denote (^{15}N,^{13}C)-labeled nucleotides.

Detection of the iminoproton of each labeled site was then attempted to determine whether it was involved in hydrogen bonding. The iminoproton signal of U8, although weak, could be observed (Fig. 3a). Judging from its low-field chemical shift, this signal suggests the involvement of the U8 residue in base pairing. The iminoproton of G(L2) was also observed, indicating that it took part in hydrogen bonding (Fig. 3b). The high-field chemical shift (10.92 ppm) of the G(L2) iminoproton signal probably indicates that the G(L2) residue formed part of an irregular base pair. Although iminoproton signals for G(L3) and U(L4) were not clearly observed in the absence of Mg^{2+}, they became apparent when Mg^{2+} was added up to 15 mM (Fig. 4a). Even though the latter two iminoproton signals are weak, both protons are thought to have been involved in hydrogen bonding, because the chemical shifts lay in the low magnetic field range (12.29 and 13.19 ppm, respectively). They were discriminated from each other by (G or U)-selective decoupling of the iminoprotons by irradiation with weak power. Figure 4, b and c, respectively, shows the [^{15}N]^1H HMQC spectra in which the iminoprotons of G and U are selectively decoupled from ^{15}N. These spectra proved that the signals at 13.19 and 12.29 ppm were respectively those of the iminoprotons of U(L4) and G(L3). Although it is possible that G(L5) might form a Watson-Crick base pair with C(L11) to make "the shortest" T stem as described in Wolstenholme *et al.* (*10*), no clear iminoproton signal was observed for G(L5) even in the presence of Mg^{2+} (Fig. 3c).

DISCUSSION

Several methods of site-specific labeling of RNA samples have been devised to facilitate the NMR analyses of RNA. It has recently been shown that segmental labeling can be achieved by ligation of RNase H-cleaved fragments with DNA ligase (*22*). We previously demonstrated the possibility of obtaining biologically active tRNA molecules in sufficient amount for NMR measurement by ligation of

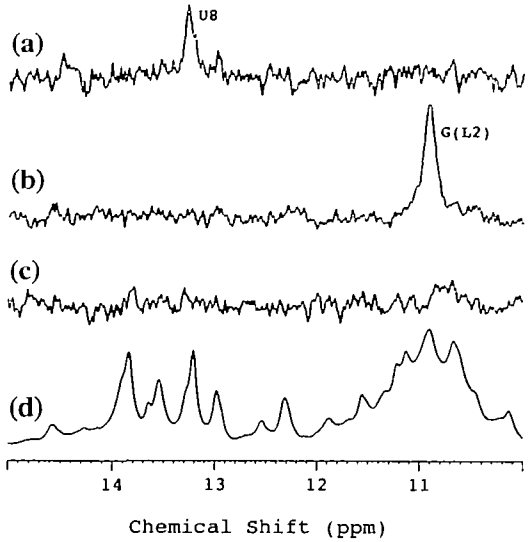

Fig. 3. **1D spectra of synthetic *A. suum* mt tRNAs^{Met} recorded at 283 K.** HMQC spectra of the tRNAs labeled at positions U8 (a), G(L2) (b), and G(L5) (c), and the normal spectrum of the unlabeled tRNA (d) are shown.

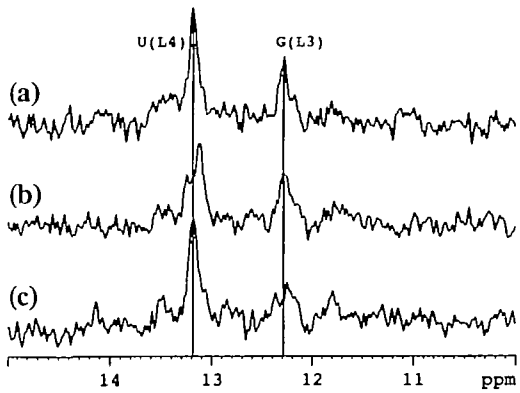

Fig. 4. **1D HMQC spectra of [G(L3),U(L4)]-labeled *A. suum* mt tRNA^{Met} recorded at 303 K.** The HMQC spectrum is shown in (a); the iminoproton signal for G (b) or U (c) was selectively decoupled from ^{15}N (5,800 Hz for G or 6,600 Hz for U) by weak irradiation.

chemically synthesized RNA fragments with RNA ligase (*16*). In the present work, specific residues were labeled using the RNA ligation method. Site-specific labeling is useful for the assignment of a specific site in an RNA and determining the local structure around the labeled site. It should be noted that the method used here is applicable to single-residue labeling of RNA, because, while a small RNA substrate like a mononucleotide cannot be ligated with DNA ligase, it can be ligated with RNA ligase. The amount of labeled nucleotide needed in this method is considerably less than that required in chemical synthesis of a labeled RNA. About 10 mg of labeled monomer is necessary for single-residue labeling by chemical synthesis at a scale of 1 μmol. For example, chemical synthesis at a scale of 1 μmol yielded about 1.3 mg of *A. suum* mt tRNA^{Met} (*18*), whereas, 1.3 mg of G(L5)-labeled tRNA was prepared using only 60 μg of [^{15}N,^{13}C]Gp by the present method.

The iminoproton signals of tRNAs labeled at a single residue could be assigned easily and unambiguously, while those labeled at two residues (one G and one U) were also assigned easily by means of chemical shifts of ^{15}N. They could be distinguished by (G or U)-selective decoupling of the iminoprotons by irradiation with weak power. Again, G(L5) gave no detectable imino proton signals, indicating that even "the shortest" T-stem with the L5-L11 pairing does not exist. Because the iminoproton signals of G(L2), G(L3), U(L4), and U8 were weak, NOEs from those signals could not be detected. Those weak signals may provide a evidence for the existence of unstable tertiary interactions. Thus, the folding in the core region of this tRNA is probably not rigid in comparison with that of standard tRNAs. In fact, iminoproton signals involved in tertiary interactions in the core region of yeast tRNA^{Phe} (*23*), *E. coli* tRNA^{Val} (*24*) and *E. coli* tRNA^{Phe} (*25*) were not weak, and NOE signals from these signals were observed.

On the basis of the enzymatic probing data (*5, 16*) and NOE connectivity of iminoproton signals in the presumed secondary base pairs (a part of these signals were assigned; data not shown) of a nematode (*A. suum*) mt tRNA^{Met} lacing the T arm, its secondary structure had been speculated to be as shown by Fig. 1a. Hence, the tertiary interactions of the tRNA were investigated in the present study by using NMR. Together with these NMR observations and the previous data obtained by Wolstenholme *et al.* (*10*) and Watanabe *et al.* (*5*), the tertiary interactions in *A. suum* mt tRNA^{Met} were deduced with reference to those in yeast tRNA^{Phe} (Table II). To arrange the base locations according to these tertiary interactions, MD calculation was performed for the core region under the condition that neither anticodon arm nor acceptor stem was present, which resulted in the structural model shown in Fig. 5a. It is noted that the iminoproton in G(L2) was involved in hydrogen bonding (Fig. 5a), because its signal could be observed, while the iminoproton in corresponding nucleotide (G45) in yeast tRNA^{Phe} was not. Figure 5b shows the structural model for whole tRNA including the core structure shown in Fig. 5a. The model does not conflict with the results of enzymatic probing (*5, 16*) already reported by us.

The structure of the ternary complex of yeast phenylalanyl-tRNA^{Phe}, *Thermus aquaticus* EF-Tu, and GTP indicates that domain 3 of EF-Tu interacts with the T stem of tRNA^{Phe} (*26*). However, nematode mt tRNAs other than tRNAs$^{Ser}_{UCU}$ and tRNAs$^{Ser}_{UCA}$ lack the T stem. It thus seems that nematode mt EF-Tu does not recognize the T stem or that the EF-Tu has a special domain to compensate for the absent region of T arm. Thus far, the higher-order structures of various mt tRNAs have been elucidated, including mammalian mt tRNA$^{Ser}_{UCU}$ lacking D arm (*8, 27, 28*), bovine mt tRNA^{Phe} lacking the "conserved" GG and TΨCG sequences (*29*), and bovine mt tRNA$^{Ser}_{UCA}$ lacking 6-residues (*30, 31*). Their following functions have also been examined *in vitro*: the interactions of bovine mt tRNA$^{Ser}_{UCU}$ (*32*) and bovine mt tRNA^{Phe} (*33*) with the cognate aminoacyl-tRNA synthetases, the translation activities in the presence of the corresponding mRNAs, ribosomes and elongation factors of bovine mt tRNA^{Phe} (*34*) and bovine mt tRNA^{Met} (*35*) with mRNA-containing ribosome and elongation factors. However, there have been no reports concerning the structure-function relationship of nematode mt tRNA lacking the T arm, which we hope to elucidate in the near future.

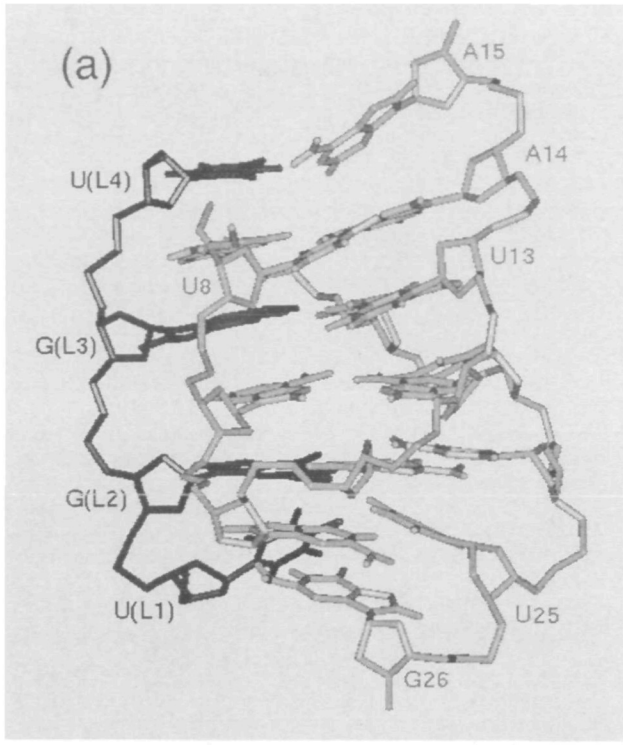

Fig. 5. **The tertiary structural model of *A. suum* mt tRNA^{Met}.** (a) The core region in the model. Residues in the TV loop are colored black. (b) Overall shape of the model. Nucleotides sensitive to RNase T_2 are colored white and those sensitive to RNase V_1 are colored black (*16*).

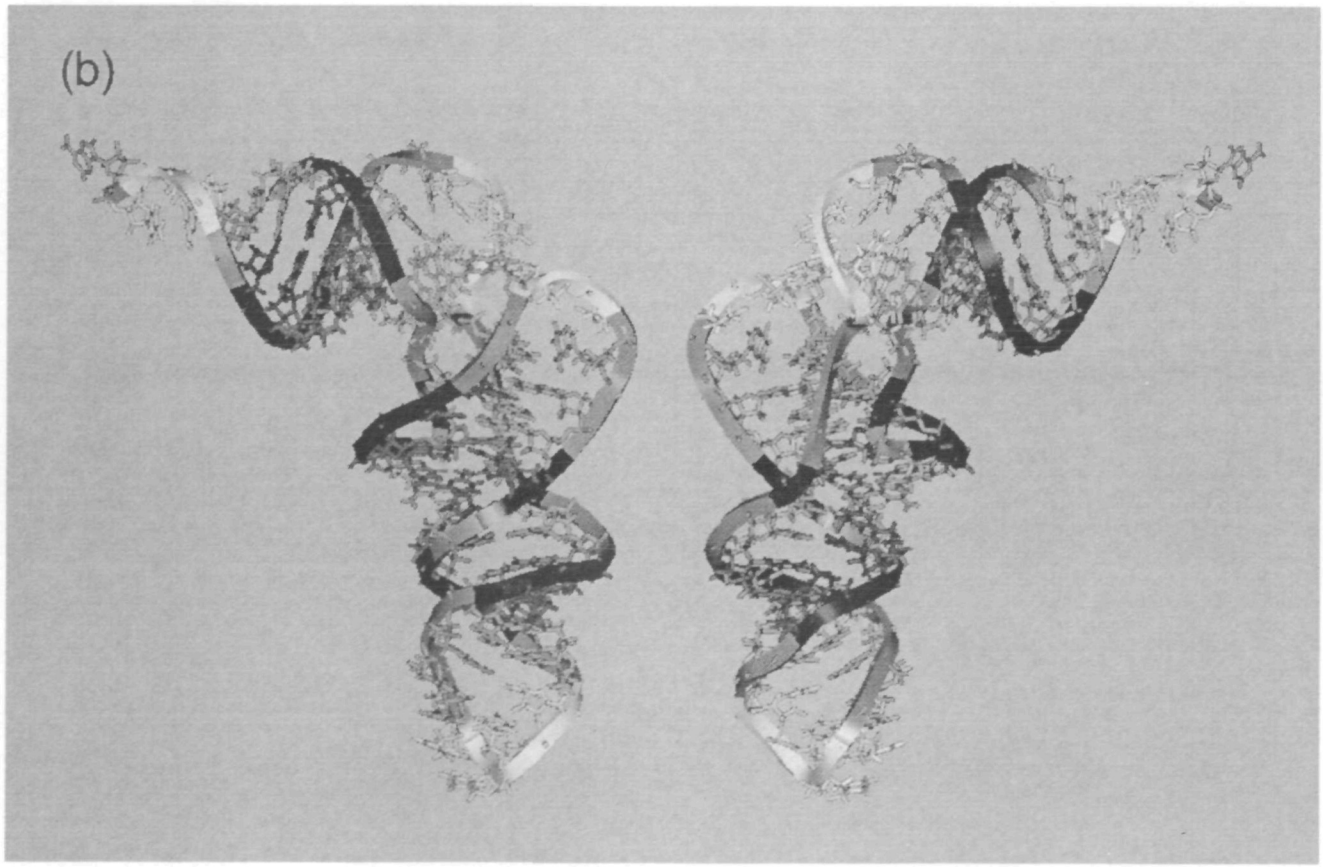

We thank H. Fukui, A. Ura, and I. Kim for their help in the preparation of labeled nucleotides, and Dr. Y. Watanabe for discussions.

REFERENCES

1. Sprinzl, M., Steegborn, C., Hubel, F., and Steinberg, S. (1996) Compilation of tRNA sequences and sequences of tRNA genes. *Nucleic Acids Res.* **24**, 68-72
2. Wolstenholme, D.R., Macfarlane, J.L., Okimoto, R., Clary, D.O., and Wahleithner, J.A. (1987) Bizarre tRNAs inferred from DNA sequences of mitochondrial genomes of nematode worms. *Proc. Natl. Acad. Sci. USA* **84**, 1324-1328
3. Okimoto, R. and Wolstenholme, D.R. (1990) A set of tRNAs that lack either the TΨC arm or the dihydrouridine arm: towards a minimal tRNA adaptor. *EMBO J.* **9**, 3405-3411
4. Okimoto, R., Chamberlin, H.M., Macfarlane, J.L., and Wolstenholme, D.R. (1991) Repeated sequence sets in mitochondrial DNA molecules of root knot nematodes (*Meloidogyne*): nucleotide sequences, genome location and potential for host-race identification. *Nucleic Acids Res.* **19**, 1619-1626
5. Watanabe, Y., Tsurui, H., Ueda, T., Furushima, R., Takamiya, S., Kita, K., Nishikawa, K., and Watanabe, K. (1994) Primary and higher order structures of nematode (*Ascaris suum*) mitochondrial tRNAs lacking either the T or D stem. *J. Biol. Chem.* **269**, 22902-22906
6. Okimoto, R., Macfarlane, J.L., Clary, D.O., and Wolstenholme, D.R. (1992) The mitochondrial genomes of two nematodes, *Caenorhabditis elegans* and *Ascaris suum*. *Genetics* **130**, 471-498
7. Watanabe, Y., Tsurui, H., Ueda, T., Furushima-Shimogawara, R., Takamiya, S., Kita, K., Nishikawa, K., and Watanabe, K. (1997) Primary sequence of mitochondrial $tRNA^{Arg}$ of a nematode *Ascaris suum*: occurrence of unmodified adenosine at the first position of the anticodon. *Biochim. Biophys. Acta* **1350**, 119-122
8. Steinberg, S. and Cedergren, R. (1994) Structural compensation in atypical mitochondrial tRNAs. *Nature Struct. Biol.* **1**, 507-510
9. Rich, A. and Kim, S.-H. (1978) The three-dimensional structure of transfer RNA. *Sci. Am.* **238**(1), 52-62
10. Wolstenholme, D.R., Okimoto, R., and Macfarlane, J.L. (1994) Nucleotide correlations that suggest tertiary interactions in the TV-replacement loop-containing mitochondrial tRNAs of the nematodes, *Caenorhabditis elegans* and *Ascaris suum*. *Nucleic Acids Res.* **22**, 4300-4306
11. Varani, G., Aboul-ela, F., and Allain, F.H.-T. (1996) NMR investigation of RNA structure. *Prog. Nucl. Magn. Reson. Spectrosc.* **29**, 51-127
12. Milligan, J.F., Groebe, D.R., Witherell, G.W., and Uhlenbeck, Q.C. (1987) Oligoribonucleotide synthesis using T7 RNA polymerase and synthetic DNA templates. *Nucleic Acids Res.* **15**, 8783-8798
13. Niconowicz, E.P., Sirr, A., Legault, P., Jucker, F.M., Baer, L.M., and Pardi, A. (1992) Preparation of ^{13}C and ^{15}N labeled RNAs for heteronuclear multi-dimensional NMR studies. *Nucleic Acids Res.* **20**, 4507-4513
14. Batey, R.T., Inada, M., Kujawinski, E., Puglisi, J.D., and Williamson, J.R. (1992) Preparation of isotopically labeled ribonucleotides for multidimensional NMR spectroscopy of RNA. *Nucleic Acids Res.* **20**, 4515-4523
15. Michnicka, M.J., Harper, J.W., and King, G.C. (1993) Selective isotopic enrichment of synthetic RNA: application to the HIV-1 TAR element. *Biochemistry* **32**, 395-400
16. Ohtsuki, T., Kawai, G., Watanabe, Y., Kita, K., Nishikawa, K., and Watanabe, K. (1996) Preparation of biologically active *Ascaris suum* mitochondrial $tRNA^{Met}$ with a TV-replacement loop by ligation of chemically synthesized RNA fragments. *Nucleic Acids Res.* **24**, 662-667
17. Nishikawa, K. and Takemura, S. (1974) Structure and function of 5S ribosomal ribonucleic acid from *Torulopsis utilis*. II. Partial digestion with ribonucleases and derivation of the complete sequence. *J. Biochem.* **76**, 925-934
18. Ohtsuki, T., Vinayak, R., Watanabe, Y., Kita, K., Kawai, G., and Watanabe, K. (1996) Automated chemical synthesis of biologically active tRNA having a sequence corresponding to *Ascaris suum* mitochondrial $tRNA^{Met}$ toward NMR mesurements. *J. Biochem.* **120**, 1070-1073
19. Plateau, P. and Guéron, M. (1982) Exchangeable proton NMR without base-line distortion, using new strong-pulse sequenses. *J. Am. Chem. Soc.* **104**, 7310-7311
20. Bax, A., Griffey, R.H., and Hawkins, B.L. (1983) Correlation of proton and nitrogen-15 chemical shifts by multiple quantum NMR. *J. Magn. Reson.* **55**, 301-315
21. Shaka, A.J., Barker, P.B., and Freeman, R. (1985) Computer-optimized decoupling scheme for wideband applications and low-level operation. *J. Magn. Reson.* **64**, 547-552
22. Xu, J., Lapham, J., and Crothers, D.M. (1996) Determining RNA solution structure by segmental isotopic labeling and NMR: application to *Caenorhabditis elegans* spliced leader RNA 1. *Proc. Natl. Acad. Sci. USA* **93**, 44-88
23. Roy, S. and Redfield, A.G. (1983) Assignment of imino proton spectra of yeast phenylalanine transfer ribonucleic acid. *Biochemistry* **22**, 1386-1390
24. Hare, D.R., Ribeiro, N.S., Wemmer, D.E., and Reid, B.R. (1985) Complete assignment of the imino protons of *Escherichia coli* valine transfer RNA: two-dimensional NMR studies in water. *Biochemistry* **24**, 4300-4306
25. Hyde, E.I. and Reid, B.R. (1985) Assignment of the low-field ^1H NMR spectrum of *Escherichia coli* $tRNA^{Phe}$ using nuclear Overhauser effects. *Biochemistry* **24**, 4307-4314
26. Nissen, P., Kjeldgaard, M., Thirup, S., Polekhina, G., Reshetnikova, L., Clark, B.F., and Nyborg, J. (1995) Crystal structure of the ternary complex of Phe-$tRNA^{Phe}$, EF-Tu, and a GTP analog. *Science* **270**, 1464-1472
27. de Bruijn, M.H.L. and Klug, A. (1983) A model for the tertiary structure of mammalian mitochondrial transfer RNAs lacking the entire "dihydrouridine" loop and stem. *EMBO J.* **2**, 1309-1321
28. Steinberg, S., Gautheret, D., and Cedergren, R. (1994) Fitting the structurally diverse animal mitochondrial $tRNAs^{Ser}$ to common three-dimensional constraints. *J. Mol. Biol.* **236**, 982-989
29. Wakita, K., Watanabe, Y., Yokogawa, T., Kumazawa, Y., Nakamura, S., Ueda, T., Watanabe, K., and Nishikawa, K. (1994) Higher-order structure of bovine mitochondrial $tRNA^{Phe}$ lacking the 'conserved' GG and TΨCG sequences as inferred by enzymatic and chemical probing. *Nucleic Acids Res.* **22**, 347-353
30. Yokogawa, T., Watanabe, Y., Kumazawa, Y., Ueda, T., Hirao, I., Miura, K., and Watanabe, K. (1991) A novel cloverleaf structure found in mammalian mitochondrial $tRNA^{Ser}$(UCN). *Nucleic Acids Res.* **19**, 6101-6105
31. Watanabe, Y., Kawai, G., Yokogawa, T., Hayashi, N., Kumazawa, Y., Ueda, T., Nishikawa, K., Hirao, I., Miura, K., and Watanabe, K. (1994) Higher-order structure of bovine mitochondrial $tRNA^{Ser}_{UCA}$: chemical modification and computer modeling. *Nucleic Acids Res.* **22**, 5378-5384
32. Ueda, T., Yotsumoto, Y., Ikeda, K., and Watanabe, K. (1992) The T-loop region of animal mitochondrial $tRNA^{Ser}$(AGY) is a main recognition site for homologous seryl-tRNA synthetase. *Nucleic Acids Res.* **20**, 2217-2222
33. Kumazawa, Y., Yokogawa, T., Hasegawa, E., Miura, K., and Watanabe, K. (1989) The aminoacylation of structurally variant phenylalanine tRNAs from mitochondria and various nonmitochondrial sources by bovine mitochondrial phenylalanyl-tRNA synthetase. *Biochim. Biophys. Acta* **264**, 13005-13011
34. Kumazawa, Y., Schwartzbach, C.J., Liao, H.X., Mizumoto, K., Kaziro, Y., Miura, K., Watanabe, K., and Spremulli, L.L. (1991) Interactions of bovine mitochondrial phenylalanyl-tRNA with ribosomes and elongation factors from mitochondria and bacteria. *Biochim. Biophys. Acta* **1090**, 167-172
35. Takemoto, C., Koike, T., Yokogawa, T., Benkowski, L., Spremulli, L.L., Ueda, T., Nishikawa, K., and Watanabe, K. (1995) The ability of bovine mitochondrial transfer RNA^{Met} to decode AUG and AUA codons. *Biochimie* **77**, 104-108
36. Ferrin, T.E., Huang, C.C., Jarvis, L.E., and Langridge, R. (1988) The midas display system. *J. Mol. Graphics* **6**, 13-27